

# Deconstruction, 2d lattice super-Yang-Mills, and the dynamical lattice spacing

Joel Giedt\*

*University of Toronto  
60 St. George St., Toronto ON M5S 1A7 Canada*

## Abstract

We study expectation values related to the dynamical lattice spacing that occurs in the recent 2d lattice super-Yang-Mills constructions of Cohen et al. [hep-lat/0307012]. The corresponding observable in the fully-quenched ensemble would appear to indicate a difficulty with the proposed continuum limit. However, we find that the same observable in the phase-quenched ensemble takes a very different, perhaps encouraging, average value. Unfortunately, we are not able to obtain results for the full theory, due to the nearly flat distribution of the complex phase of the fermion determinant in the phase-quenched ensemble.

---

\*giedt@physics.utoronto.ca

# 1 Introduction

In [1], a lattice action has been proposed by Cohen, Kaplan, Katz and Unsal (CKKU) for the (4,4) 2d  $U(k)$  super-Yang-Mills.<sup>1</sup> The Euclidean target theory action is

$$S_{(4,4)} = \int d^2x \frac{1}{g_2^2} \text{Tr} \left[ (Ds_\mu) \cdot (Ds_\mu) + \bar{\psi}_i \not{D} \psi_i + \frac{1}{4} F \cdot F + \bar{\psi}_i [(s_0 \delta_{ij} + i\gamma_3 \mathbf{s} \cdot \boldsymbol{\sigma}_{ij}), \psi_j] - \frac{1}{2} [s_\mu, s_\nu]^2 \right] \quad (1.1)$$

where  $s_\mu$  ( $\mu = 0, 1, 2, 3$ ) are hermitian scalars,  $F$  is the 2d Yang-Mills field strength, and  $\psi_i$  ( $i = 1, 2$ ) are 2d Dirac fermions, all in the adjoint representation of  $U(k)$ . In [2], some aspects of the fermion determinant were examined, with results very similar to those in [3]. We will have occasion to review those results below.

Here we will study a rather fundamental aspect of the construction: the proposed emergence of a “dynamical” lattice spacing. CKKU make use of an  $N \times N$  lattice that contains link and site fields that are  $k \times k$  matrices. The classical lattice action contains many zero-action configurations. CKKU expand the classical lattice action about a particular class of zero-action configurations (discussed below) that are characterized by a parameter  $a$ . For this reason we will refer to such a configuration as an  $a$ -configuration. In the limit  $a \rightarrow 0$ ,  $N \rightarrow \infty$ , the classical action tends to (1.1). Thus  $a$  is interpreted as a lattice spacing. However, it is dynamical as it has to do with a particular background configuration for the lattice fields. This strategy is based on the ideas of *deconstruction* [4, 5]. Studies where a partial latticization of 4d supersymmetric theories has been obtained by this approach include [6, 7].

The validity of the semi-classical expansion, about an  $a$ -configuration, rests on the assumption that it gives a good approximation to the behavior of the full lattice theory. But all  $a$ -configurations are energetically equivalent. Furthermore, there exist other zero action configurations that do not fall into the  $a$ -configuration class (shown below). Finally, it is important that the fluctuations about the  $a$ -configuration be in some sense subdominant. For these reasons, CKKU deform the action by adding an  $a$ -dependent potential that favors the  $a$ -configuration. The “continuum limit” then includes sending  $a \rightarrow 0$  in this potential. Although this deformation breaks the exact lattice supersymmetry, it is rendered harmless by scaling the relative strength of the deformation potential to zero in the thermodynamic limit. For this reason it has been argued by CKKU that the quantum continuum limit is nothing but the target theory. Based on the symmetries of the undeformed theory, it would appear that the target theory is obtained without the need for fine-tuning. For further details, we refer the reader to [1], as well as the articles leading up to it [8, 9].

The deconstruction method for latticizing a continuum target theory does not require fermions or supersymmetry. The bosonic system (i.e., setting all lattice fermions to zero)

---

<sup>1</sup>The (4,4) 2d  $U(k)$  super-Yang-Mills is best defined as the dimensional reduction of  $\mathcal{N} = 1$  6d  $U(k)$  super-Yang-Mills; the notation “(4,4)” denotes the number of left and right 2d chirality supercharges.

contained in the model of CKKU already has the interesting feature of a deconstructed lattice Yang-Mills. The same semi-classical arguments yield  $U(k)$  Yang-Mills with 4 adjoint scalars; that is, the bosonic part of (1.1). In the present article we will investigate the validity of the semi-classical argument in both this bosonic theory and in the full supersymmetric theory. We will take into account quantum effects, estimating key expectation values by means of Monte Carlo simulation.

We now summarize the content and results of the rest of the article:

- In the next section we introduce the essential features of the bosonic part of the CKKU construction that will be needed for the subsequent discussion. We then study the classical minima of the undeformed and deformed actions in Section 3. We show that in the undeformed theory there is a vast number of zero-action configurations. We further show that the deformation leaves only a particular  $a$ -configuration with zero action, modulo gauge equivalences.
- In Section 4 we outline the methods and results of our lattice simulation for the bosonic system. We find that the expectation values do not agree with the semi-classical predictions based on energetic arguments. In Section 5 we suggest an interpretation of these results in terms of the analysis of Section 3. We find that the simulation results are consistent with entropic effects dominating the expectation values.
- In Section 6 we attempt to include the effects of fermions. We show that this is crucial for understanding the dynamical lattice spacing in the supersymmetric theory, because the fermion matrix is highly singular for the zero-action configurations of the undeformed theory. Difficulties are encountered because of the complex phase of the fermion determinant. We present results for expectation values in the phase-quenched ensemble. However, we are unable to obtain reliable expectation values for the full theory, via phase reweighting, due to the nearly flat distribution of the complex phase.
- In Section 7 we make some concluding remarks. In the Appendix, we provide a brief review of the  $\mathcal{N} = 4$  4d super-Yang-Mills moduli space, which arises in the discussion of Section 3.

## 2 Quiver lattice Yang-Mills

For CKKU, the starting point is the Euclidean  $\mathcal{N} = 1$  6d  $U(kN^2)$  super-Yang-Mills. In our considerations of the bosonic theory, the starting point will be just the Euclidean 6d  $U(kN^2)$  Yang-Mills. In either case, the action is dimensionally reduced to 0d to obtain a  $U(kN^2)$  matrix model. The matrix model naturally possesses  $SO(6)$  Euclidean invariance. Next we note  $SO(6) \supset SO(2) \times SO(2) \supset Z_N \times Z_N$ . CKKU have identified a homomorphic embedding of  $Z_N \times Z_N$  into the  $U(kN^2)$  gauge symmetry group. Using this, a  $Z_N \times Z_N$  orbifold projection is performed to obtain a  $U(k)^{N^2}$  0d *quiver*, or, *product group* theory.<sup>2</sup> In

---

<sup>2</sup>Quiver theories were originally studied many years ago in other contexts [10, 11].

every respect we follow CKKU, except that in the bosonic theory we have set all fermions to zero. For details of the matrix model and orbifold projection, we refer the reader to [1]. In the interests of brevity, we will only give the final results. The *undeformed* bosonic lattice action is

$$\begin{aligned}
S_0 = & \frac{1}{g^2} \text{Tr} \sum_{\mathbf{n}} \left[ \frac{1}{2} (x_{\mathbf{n}-\hat{\mathbf{i}}}^\dagger x_{\mathbf{n}-\hat{\mathbf{i}}} - x_{\mathbf{n}} x_{\mathbf{n}}^\dagger + y_{\mathbf{n}-\hat{\mathbf{j}}}^\dagger y_{\mathbf{n}-\hat{\mathbf{j}}} - y_{\mathbf{n}} y_{\mathbf{n}}^\dagger + z_{\mathbf{n}}^\dagger z_{\mathbf{n}} - z_{\mathbf{n}} z_{\mathbf{n}}^\dagger)^2 \right. \\
& + 2(x_{\mathbf{n}} y_{\mathbf{n}+\hat{\mathbf{i}}} - y_{\mathbf{n}} x_{\mathbf{n}+\hat{\mathbf{j}}}) (y_{\mathbf{n}+\hat{\mathbf{i}}}^\dagger x_{\mathbf{n}}^\dagger - x_{\mathbf{n}+\hat{\mathbf{j}}}^\dagger y_{\mathbf{n}}^\dagger) \\
& + 2(y_{\mathbf{n}} z_{\mathbf{n}+\hat{\mathbf{j}}} - z_{\mathbf{n}} y_{\mathbf{n}}) (z_{\mathbf{n}+\hat{\mathbf{j}}}^\dagger y_{\mathbf{n}}^\dagger - y_{\mathbf{n}}^\dagger z_{\mathbf{n}}^\dagger) \\
& \left. + 2(z_{\mathbf{n}} x_{\mathbf{n}} - x_{\mathbf{n}} z_{\mathbf{n}+\hat{\mathbf{i}}}) (x_{\mathbf{n}}^\dagger z_{\mathbf{n}}^\dagger - z_{\mathbf{n}+\hat{\mathbf{i}}}^\dagger x_{\mathbf{n}}^\dagger) \right] \quad (2.1)
\end{aligned}$$

The fermionic lattice action will be given in Section 6, where we will examine the effects of the fermion determinant. In (2.1),  $x_{\mathbf{m}}, y_{\mathbf{m}}, z_{\mathbf{m}}$  are bosonic lattice fields that are  $k \times k$  unconstrained complex matrices;  $\mathbf{m} = (m_1, m_2)$  labels points on an  $N \times N$  lattice, and  $\hat{\mathbf{i}} = (1, 0), \hat{\mathbf{j}} = (0, 1)$  are unit vectors. The  $U(k)^{N^2}$  symmetry is nothing but the local  $U(k)$  symmetry of the lattice action  $S_0$ , with link bosons  $x_{\mathbf{m}}$  in the  $\hat{\mathbf{i}}$  direction, link bosons  $y_{\mathbf{m}}$  in the  $\hat{\mathbf{j}}$  direction, and sites bosons  $z_{\mathbf{m}}$ , all transforming in the usual manner:

$$x_{\mathbf{m}} \rightarrow \alpha_{\mathbf{m}} x_{\mathbf{m}} \alpha_{\mathbf{m}+\hat{\mathbf{i}}}^\dagger, \quad y_{\mathbf{m}} \rightarrow \alpha_{\mathbf{m}} y_{\mathbf{m}} \alpha_{\mathbf{m}+\hat{\mathbf{j}}}^\dagger, \quad z_{\mathbf{m}} \rightarrow \alpha_{\mathbf{m}} z_{\mathbf{m}} \alpha_{\mathbf{m}}^\dagger \quad (2.2)$$

Canonical mass dimension 1 is assigned to  $x_{\mathbf{m}}, y_{\mathbf{m}}, z_{\mathbf{m}}$ , whereas  $g$  has mass dimension 2.

Although  $S_0$  is a lattice action that describes a statistical system with interesting features, it is not in any obvious way related to a 2d continuum field theory (1.1). As will be explained below,  $S_0 \geq 0$  and a vast number of nontrivial solutions to  $S_0 = 0$  exist, not all of which are gauge equivalent. In fact, the space of minimum action configurations, or *moduli space*, is a multi-dimensional noncompact manifold with various *branches* (classes of configurations). For this reason it is difficult to say what a ‘‘continuum limit’’ might be; for there exists an infinite number of energetically equivalent configurations about which to expand, not all of which are gauge equivalent.

A surprising result—pointed out by CKKU, and based on ideas from deconstruction—is obtained if one expands about the *a-configuration*

$$x_{\mathbf{m}} = \frac{1}{a\sqrt{2}} \mathbf{1}, \quad y_{\mathbf{m}} = \frac{1}{a\sqrt{2}} \mathbf{1}, \quad z_{\mathbf{m}} = 0, \quad \forall \mathbf{m} \quad (2.3)$$

keeping  $g_2 = ga$  and  $L = Na$  fixed, treating  $a$  as small. (It is easy to see that  $S_0 = 0$  for this configuration.) That is, we associate  $a$  with a lattice spacing (mass dimensions -1), even though it arises originally from a specific background field configuration. In this case, one finds that the classical continuum limit is nothing but the bosonic part of (1.1), which is a variety of 2d  $U(k)$  Yang-Mills with adjoint scalars. In the case of the supersymmetric quiver theory of CKKU, where fermions are present, one obtains (1.1) in full; i.e., (4,4) 2d  $U(k)$  super-Yang-Mills.

The trick is how to make the configuration (2.3) energetically preferred without destroying all of the pleasing symmetry properties of the theory. (This is particularly true in the supersymmetric case.) In the quantum analysis, we must address the more delicate complication of entropy as well. CKKU suggest a deformation of the bosonic action in an effort to stabilize the theory near the  $a$ -configuration (2.3):

$$S_B = S_0 + S_{\text{SB}} \tag{2.4}$$

$$S_{\text{SB}} = \frac{a^2 \mu^2}{2g^2} \sum_{\mathbf{n}} \text{Tr} \left[ \left( x_{\mathbf{n}} x_{\mathbf{n}}^\dagger - \frac{1}{2a^2} \right)^2 + \left( y_{\mathbf{n}} y_{\mathbf{n}}^\dagger - \frac{1}{2a^2} \right)^2 + \frac{2}{a^2} z_{\mathbf{n}} z_{\mathbf{n}}^\dagger \right] \tag{2.5}$$

Here the strength of the deformation is determined by the quantity  $\mu$ , which has mass dimension 1. It is clear that the configuration (2.3) minimizes  $S_{\text{SB}}$ . (Other configurations that minimize  $S_0$  and  $S_{\text{SB}}$  will be discussed below.) Unfortunately, in the supersymmetric version of CKKU, the deformation  $S_{\text{SB}}$  breaks the exact supersymmetry of their original lattice action (hence the subscript ‘‘SB’’ = Symmetry Breaking). For this reason they demand that the strength of  $S_{\text{SB}}$  relative to  $S_0$ , conveyed by  $\mu^2$ , be scaled to zero in the thermodynamic limit. Thus we are interested in the effects of the deformation subject to this scaling.

In much of what follows we will specialize to the case of  $U(2)$ . This is merely because it is the simplest case and the most efficient to simulate. In this special case,  $x_{\mathbf{m}}, y_{\mathbf{m}}, z_{\mathbf{m}}$  will be unconstrained  $2 \times 2$  complex matrices.

### 3 The classical analysis

Here details are given of the classical analysis of the minima of the action  $S_B$ . In Section 3.1 we consider the undeformed action  $S_0$ ; then in Section 3.2 we consider the modifications induced by the deformation  $S_{\text{SB}}$ , which has the effect of lifting some flat directions in moduli space. Through understanding this classical picture, naive expectations of what will occur in the quantum theory, based on energetics, can be formulated.

#### 3.1 Undeformed theory

Here we neglect  $S_{\text{SB}}$  and examine the minima of  $S_0$ . Note that (2.1) is a sum of terms of the form  $\text{Tr} AA^\dagger$  (the first line involves squares of hermitian matrices). Thus  $S_0 \geq 0$  with  $S_0 = 0$  iff the following equations hold true:

$$x_{\mathbf{n}-\hat{\mathbf{i}}}^\dagger x_{\mathbf{n}-\hat{\mathbf{i}}} - x_{\mathbf{n}} x_{\mathbf{n}}^\dagger + y_{\mathbf{n}-\hat{\mathbf{j}}}^\dagger y_{\mathbf{n}-\hat{\mathbf{j}}} - y_{\mathbf{n}} y_{\mathbf{n}}^\dagger + [z_{\mathbf{n}}^\dagger, z_{\mathbf{n}}] = 0 \tag{3.1}$$

$$x_{\mathbf{n}} y_{\mathbf{n}+\hat{\mathbf{i}}} - y_{\mathbf{n}} x_{\mathbf{n}+\hat{\mathbf{j}}} = y_{\mathbf{n}} z_{\mathbf{n}+\hat{\mathbf{j}}} - z_{\mathbf{n}} y_{\mathbf{n}} = z_{\mathbf{n}} x_{\mathbf{n}} - x_{\mathbf{n}} z_{\mathbf{n}+\hat{\mathbf{i}}} = 0 \tag{3.2}$$

together with the h.c. of (3.2). The set of solutions is the moduli space of the undeformed theory.

### 3.1.1 Zeromode branch

To begin a study of the moduli space, we isolate the zero momentum modes:  $x_{\mathbf{n}} \equiv x \forall \mathbf{n}$ , etc. Then Eqs. (3.1) and (3.2) reduce to

$$\begin{aligned} [x^\dagger, x] + [y^\dagger, y] + [z^\dagger, z] &= 0 \\ [x, y] = [y, z] = [z, x] &= 0 \end{aligned} \quad (3.3)$$

together with the h.c. of the second line of (3.3). Eqs. (3.3) may be recognized as nothing but the *D-flatness* and *F-flatness* constraints that describe the moduli space associated with the classical scalar vacuum of  $\mathcal{N} = 4$  4d super-Yang-Mills.<sup>3</sup> The equations are invariant with respect to the global gauge transformation

$$x \rightarrow \alpha x \alpha^\dagger, \quad y \rightarrow \alpha y \alpha^\dagger, \quad z \rightarrow \alpha z \alpha^\dagger \quad (3.4)$$

Then it is well-known that solutions to (3.3) consist of  $x, y, z$  that lie in a Cartan subalgebra of  $U(k)$ ; the proof is reviewed in Appendix A. The global gauge transformations (3.4) allow one to change to a basis where this Cartan subalgebra has a diagonal realization. Thus one can think of the moduli space as the set of all possible diagonal matrices  $x, y, z$ , and all global gauge transformations (3.4) of this set.

In particular, the zeromode moduli space of the undeformed  $U(2)$  theory is completely described by

$$x = x^0 + x^3 \sigma^3, \quad y = y^0 + y^3 \sigma^3, \quad z = z^0 + z^3 \sigma^3, \quad (3.5)$$

with arbitrary complex numbers  $x^0, x^3, y^0, y^3, z^0, z^3$ , together with  $U(2)$  transformations of these solutions.

Eqs. (3.1) and (3.2) also have non-zeromode solutions. We do not attempt to present an exhaustive account of them. We will merely point out a few such branches in order to illustrate that the undeformed theory has a very complicated and large set of  $S_0 = 0$  configurations. This observation will be relevant to our interpretation of the simulation results in Section 5.

### 3.1.2 $x_{\mathbf{m}} = y_{\mathbf{m}} = 0$ non-zeromode branch

We have the very “large” branch of moduli space described by

$$x_{\mathbf{m}} = y_{\mathbf{m}} = 0, \quad z_{\mathbf{m}} = z_{\mathbf{m}}^0 + z_{\mathbf{m}}^3 \sigma^3, \quad \forall \mathbf{m} \quad (3.6)$$

Again,  $z_{\mathbf{m}}^0, z_{\mathbf{m}}^3$  are arbitrary complex numbers. Furthermore,  $z_{\mathbf{m}}$  is a site variable and thus transforms independently at each site as

$$z_{\mathbf{m}} \rightarrow \alpha_{\mathbf{m}} z_{\mathbf{m}} \alpha_{\mathbf{m}}^\dagger \quad (3.7)$$

---

<sup>3</sup>We thank Erich Poppitz for pointing this out to us, as well as the branch of moduli space (3.6) given below.

It can be seen that this branch affords a vast number of solutions to (3.1) and (3.2); there are  $N^2$  such solutions, modulo choices for  $z_{\mathbf{m}}^0, z_{\mathbf{m}}^3 \in \mathbf{C}$  and gauge equivalences. We will argue below that an understanding of the entropic effects that result from this branch is necessary to understanding expectation values in the quantum theory—even when a potential is introduced which gives these configurations nonvanishing action.

### 3.1.3 $z_{\mathbf{n}} = 0$ non-zeromode branch

Another branch in moduli space is the following. First we set  $z_{\mathbf{n}} = 0, \forall \mathbf{n}$ , and introduce Fourier space variables

$$x_{\mathbf{n}} = \frac{1}{N} \sum_{\mathbf{k}} \omega^{\mathbf{k} \cdot \mathbf{n}} f_{\mathbf{k}}, \quad y_{\mathbf{n}} = \frac{1}{N} \sum_{\mathbf{k}} \omega^{\mathbf{k} \cdot \mathbf{n}} g_{\mathbf{k}}, \quad \omega = \exp(2\pi i/N) \quad (3.8)$$

where  $\mathbf{k} = (k_1, k_2)$  and  $k_1, k_2 \in [0, 1, \dots, N-1]$ . Then taking into account  $z_{\mathbf{n}} = 0$ , the conditions (3.1) and (3.2) are equivalent to:

$$\begin{aligned} 0 &= \sum_{\mathbf{k}} \left( \omega^{\hat{i}\ell} f_{\mathbf{k}}^{\dagger} f_{\mathbf{k}-\ell} - f_{\mathbf{k}} f_{\mathbf{k}+\ell}^{\dagger} + \omega^{\hat{j}\ell} g_{\mathbf{k}}^{\dagger} g_{\mathbf{k}-\ell} - g_{\mathbf{k}} g_{\mathbf{k}+\ell}^{\dagger} \right) \\ 0 &= \sum_{\mathbf{k}} \left( \omega^{-\hat{i}(\ell+\mathbf{k})} f_{\mathbf{k}} g_{-\mathbf{k}-\ell} - \omega^{\hat{j}\mathbf{k}} g_{-\mathbf{k}-\ell} f_{\mathbf{k}} \right) \end{aligned} \quad (3.9)$$

for all  $\ell = (\ell_1, \ell_2)$  and  $\ell_1, \ell_2 \in [0, 1, \dots, N-1]$ . Next we turn off all modes except one for both  $f_{\mathbf{k}}$  and  $g_{\mathbf{k}}$ :

$$f_{\mathbf{k}} = \delta_{\mathbf{k}, \mathbf{k}'} f_{\mathbf{k}'}, \quad g_{\mathbf{k}} = \delta_{\mathbf{k}, -\mathbf{k}'} g_{-\mathbf{k}'} \quad (3.10)$$

Here and below, *no* sum over  $\mathbf{k}'$  is implied. When substituted into (3.9), only 2 nontrivial conditions survive:

$$0 = [f_{\mathbf{k}'}^{\dagger}, f_{\mathbf{k}'}] + [g_{-\mathbf{k}'}^{\dagger}, g_{-\mathbf{k}'}], \quad 0 = f_{\mathbf{k}'} g_{-\mathbf{k}'} - \omega^{(\hat{i}+\hat{j}) \cdot \mathbf{k}'} g_{-\mathbf{k}'} f_{\mathbf{k}'} \quad (3.11)$$

For the  $U(2)$  case, we find that solutions exist if  $\omega^{(\hat{i}+\hat{j}) \cdot \mathbf{k}'} = \pm 1$ . We already know from the zeromode considerations that for  $\omega^{(\hat{i}+\hat{j}) \cdot \mathbf{k}'} = 1$  we have solutions for  $f_{\mathbf{k}'}, g_{-\mathbf{k}'}$  diagonal matrices. In the case of  $\omega^{(\hat{i}+\hat{j}) \cdot \mathbf{k}'} = -1$  it is easy to see that there are solutions, say, of the form

$$f_{\mathbf{k}'} = z_f \sigma^3, \quad g_{-\mathbf{k}'} = z_g (\sigma^1 + b \sigma^2), \quad z_f, z_g \in \mathbf{C}, \quad b \in \mathbf{R} \quad (3.12)$$

There are many values of  $\mathbf{k}'$  for which  $\omega^{(\hat{i}+\hat{j}) \cdot \mathbf{k}'} = \pm 1$ . For  $N$  even these are

$$k'_1 + k'_2 = 0, \frac{N}{2}, N, \frac{3N}{2} \quad (3.13)$$

For  $N$  odd,  $k'_1 + k'_2 = 0, N$  are allowed and in the cases where

$$k'_1 + k'_2 = \frac{N \pm 1}{2}, \frac{3(N \pm 1)}{2} \quad (3.14)$$

(3.12) yield approximate solutions to (3.11), with an error of order  $1/N$ . Thus in the  $N \rightarrow \infty$  limit the number of  $S_0 = 0$  configurations in this class is vast; in fact, it is easy to check that the number of such configurations is approximately  $2N$ , modulo gauge equivalences and various choices for the constants in (3.12).

### 3.2 Deformed theory

Now we consider the supersymmetry breaking deformation  $S_{\text{SB}}$  introduced by CKKU. To see its effect it is handy to rewrite the quantities that appear in it. Recall that  $x_{\mathbf{m}}$  is a complex  $2 \times 2$  matrix. Dropping the subscript, we can always define

$$x = x^0 + x^a \sigma^a, \quad x^\dagger = \bar{x}^0 + \bar{x}^a \sigma^a \quad (3.15)$$

Then it is straightforward to work out ( $\mu = 0, \dots, 3$ )

$$xx^\dagger = x^\mu \bar{x}^\mu + (x^0 \bar{x}^c + \bar{x}^0 x^c + ix^a \bar{x}^b \epsilon^{abc}) \sigma^c \equiv \phi^{x,0} + \phi^{x,c} \sigma^c \equiv \phi^x \quad (3.16)$$

Note that  $\phi^{x,\mu}$  are real, and that  $\phi^{x,0}$  is positive definite. With similar definitions for  $\phi^y, \phi^z$ , the CKKU deformation is

$$\begin{aligned} S_{\text{SB}} &= \frac{a^2 \mu^2}{2g^2} \sum_{\mathbf{m}} \text{Tr} \left[ \left( \phi_{\mathbf{m}}^x - \frac{1}{2a^2} \right)^2 + \left( \phi_{\mathbf{m}}^y - \frac{1}{2a^2} \right)^2 + \frac{2}{a^2} \phi_{\mathbf{m}}^z \right] \\ &= \frac{a^2 \mu^2}{g^2} \sum_{\mathbf{m}} \left[ \left( \phi_{\mathbf{m}}^{x,0} - \frac{1}{2a^2} \right)^2 + \left( \phi_{\mathbf{m}}^{y,0} - \frac{1}{2a^2} \right)^2 + \frac{2}{a^2} \phi_{\mathbf{m}}^{z,0} \right. \\ &\quad \left. + \sum_a [(\phi_{\mathbf{m}}^{x,a})^2 + (\phi_{\mathbf{m}}^{y,a})^2] \right] \end{aligned} \quad (3.17)$$

It can be seen that the deformation drives  $\phi_{\mathbf{m}}^{x,a}, \phi_{\mathbf{m}}^{y,a}, \phi_{\mathbf{m}}^{z,0}$  toward the origin, and  $\phi_{\mathbf{m}}^{x,0}, \phi_{\mathbf{m}}^{y,0}$  toward  $1/2a^2$ . When  $\phi_{\mathbf{m}}^{z,0} = 0$ , it is easy to see that  $\phi_{\mathbf{m}}^{z,a} = 0$  identically.

To continue the analysis, it is convenient to rescale to dimensionless quantities using the parameter  $a$ :

$$\hat{g} = ga^2, \quad \hat{\mu} = \mu a, \quad \hat{\phi}_{\mathbf{m}}^x = a^2 \phi_{\mathbf{m}}^x, \quad \hat{x}_{\mathbf{m}} = ax_{\mathbf{m}}, \quad \text{etc.} \quad (3.18)$$

Then

$$S_{\text{SB}} = \frac{\hat{\mu}^2}{\hat{g}^2} \sum_{\mathbf{m}} \left[ \left( \hat{\phi}_{\mathbf{m}}^{x,0} - \frac{1}{2} \right)^2 + \left( \hat{\phi}_{\mathbf{m}}^{y,0} - \frac{1}{2} \right)^2 + 2\hat{\phi}_{\mathbf{m}}^{z,0} + \sum_a [(\hat{\phi}_{\mathbf{m}}^{x,a})^2 + (\hat{\phi}_{\mathbf{m}}^{y,a})^2] \right] \quad (3.19)$$

For any value of the lattice spacing  $a$ , the minimum of  $S_{\text{SB}}$  is obtained iff

$$\hat{\phi}_{\mathbf{m}}^{x,0} = \hat{\phi}_{\mathbf{m}}^{y,0} = \frac{1}{2}, \quad \hat{\phi}_{\mathbf{m}}^{z,0} = \hat{\phi}_{\mathbf{m}}^{x,a} = \hat{\phi}_{\mathbf{m}}^{y,a} = 0, \quad \forall \mathbf{m} \quad (3.20)$$



The conditions involving  $x_{\mathbf{m}}$  are just

$$\hat{x}_{\mathbf{m}}^{\mu} \hat{x}_{\mathbf{m}}^{\mu} = \frac{1}{2}, \quad \hat{x}_{\mathbf{m}}^0 \hat{x}_{\mathbf{m}}^c + \hat{x}_{\mathbf{m}}^c \hat{x}_{\mathbf{m}}^0 + i \hat{x}_{\mathbf{m}}^a \hat{x}_{\mathbf{m}}^b \epsilon^{abc} = 0 \quad (3.21)$$

Let us examine what additional constraint this places on classical solutions to  $S = 0$ , beyond the restrictions of the undeformed theory.

First we note that neither of the non-zero mode branches discussed in Section 3.1 above are minima of  $S_{\text{SB}}$ . Thus we pass on to the zero mode configurations (3.5). Eqs. (3.21) then imply that (3.5) is restricted to the form

$$\hat{x} = \frac{e^{i\gamma_x}}{\sqrt{2}} \text{diag} (e^{i\varphi_x}, e^{-i\varphi_x}) \quad (3.22)$$

and global gauge transformations of this. That is,  $\hat{x}$  is restricted to be an element of the maximal abelian subgroup  $U(1)^2$  of  $U(2)$ , up to an overall factor of  $1/\sqrt{2}$ . Similarly, we have for  $\hat{y}$ ,

$$\hat{y} = \frac{e^{i\gamma_y}}{\sqrt{2}} \text{diag} (e^{i\varphi_y}, e^{-i\varphi_y}) \quad (3.23)$$

Finally,  $\hat{\phi}_{\mathbf{m}}^{z,0} = 0$  implies  $z_{\mathbf{m}}^{\mu} \bar{z}_{\mathbf{m}}^{\mu} = 0$ , which has the unique solution  $z_{\mathbf{m}} = 0$ ,  $\forall \mathbf{m}$ .

Apart from global obstructions that are essentially Polyakov loops in the  $\hat{\mathbf{i}}$  or  $\hat{\mathbf{j}}$  directions, the configuration (3.22) and (3.23) can be gauged away. It is straightforward to verify that the required gauge transformation is (2.2) with

$$\alpha_{m_1, m_2} = e^{i(m_1\gamma_x + m_2\gamma_y)} \times \text{diag} (e^{i(m_1\varphi_x + m_2\varphi_y)}, e^{-i(m_1\varphi_x + m_2\varphi_y)}) \quad (3.24)$$

This sets all  $\hat{x}_{\mathbf{m}}, \hat{y}_{\mathbf{m}}$  to unity except at the ‘‘boundaries’’:

$$\begin{aligned} \hat{x}_{N, m_2} &= \frac{e^{iN\gamma_x}}{\sqrt{2}} \text{diag} (e^{iN\varphi_x}, e^{-iN\varphi_x}), \quad \forall m_2 \\ \hat{y}_{m_1, N} &= \frac{e^{iN\gamma_y}}{\sqrt{2}} \text{diag} (e^{iN\varphi_y}, e^{-iN\varphi_y}), \quad \forall m_1 \end{aligned} \quad (3.25)$$

For most purposes, we do not expect such vacua to distinguish themselves from the trivial vacua in the thermodynamic limit. In any case, global features such as these are typical of classical vacua of other lattice Yang-Mills formulations, such as the Wilson action. In our simulation study we will avoid this issue by restricting our attention to the expectation value of a quantity that is independent of these angles.

## 4 Simulation of the bosonic theory

The emergence of the effective lattice theory relies upon the assumption that fluctuations about this classical minimum are small, and that the equations (3.20) are a good approximation to the corresponding expectation values in the quantum theory. For this reason we

study

$$\langle \hat{\phi}_{\mathbf{m}}^{x,0} \rangle = \langle \hat{x}_{\mathbf{m}}^{\mu} \hat{x}_{\mathbf{m}}^{\mu} \rangle = \left\langle \frac{1}{2} \text{Tr} (\hat{x}_{\mathbf{m}} \hat{x}_{\mathbf{m}}^{\dagger}) \right\rangle \quad (4.1)$$

in our simulations, and compare the expectation values to the classical prediction (3.20).

## 4.1 Scaling

We study (4.1) along a naive scaling trajectory:

$$g_2 = a^{-1} \hat{g}(a) = \text{fixed} \quad (4.2)$$

That is, we hold the bare coupling in physical units,  $g_2$ , fixed; this is equivalent to neglecting its anomalous dimension. The dimensionless bare coupling  $\hat{g}$  is then a function of  $a$  that vanishes linearly with  $a$  as the UV cutoff is removed.

With regard to  $\hat{\mu}$  we follow the instructions of CKKU: we send the dimensionless coefficient  $\hat{\mu}$  of the deformation  $S_{\text{SB}}$  to zero as  $1/N$  while increasing  $N$ .

$$\hat{\mu}^{-1} = cN, \quad c = \mathcal{O}(1) \quad (4.3)$$

This is equivalent to scaling  $\mu = 1/cL$ , where  $c$  is a constant and  $L = Na$  is the extent of the system.

In the rescaled variables (3.18), the coefficient of the undeformed action is  $1/\hat{g}^2$ , whereas the coefficient of the deformation is  $\hat{\mu}^2/\hat{g}^2$ , as can be seen from (3.19). Thus it is that the relative strength of the deformation vanishes in the thermodynamic limit, when (4.3) is imposed.

We perform these scalings for a sequence of decreasing values of  $a$ . That is, we study the thermodynamic limit for fixed values of  $a$ . We then extrapolate toward  $a = 0$  to obtain the continuum limit.

The physical length scales are set by  $g_2^{-1}$  and the system size  $L = Na$ . To keep discretization effects to a minimum we would like to take  $g_2^{-1} \gg a$ . Equivalently,  $\hat{g}^{-1} \gg 1$ . On the other hand we are most interested in what happens at large or infinite volume. To render finite volume effects negligible would require  $g_2^{-1} \ll L$ . Equivalently,  $\hat{g}^{-1} \ll N$ . In the simulations we study the system for various choices of  $\hat{g}^{-1}$  and  $N$ . We extrapolate to the regime  $1 \ll \hat{g}^{-1} \ll N$ , but often violate the bounds  $1 \leq \hat{g}^{-1} \leq N$  for specific points where measurements are taken. The reason for this is that data outside the optimal window  $1 \ll \hat{g}^{-1} \ll N$  is informative to the extrapolation.

## 4.2 Sampling procedure

We update the system using a multi-hit Metropolis algorithm. We attempt to update a single site or link field 10 times before moving to the next, with an acceptance rate of approximately 50 percent for a single hit. We find that this minimizes autocorrelations while

maintaining program efficiency. We have examined autocorrelations and the dependence of our observables on initial conditions. These studies have led us to make 500 thermalization sweeps after a random initialization, and 100 updating sweeps between each sample. 1/2 to 2 percent standard errors result from accumulating 1000 samples at each data point.

### 4.3 Results

In Fig. 1 we show  $\langle \hat{\phi}_{\mathbf{m}}^{x,0} \rangle$  [cf. (4.1)] as a function of  $N$  for various values of  $\hat{g}^{-1}$ , having set  $c = 1$  in (4.3). Doubling  $\hat{g}^{-1}$  is equated with halving the lattice spacing, according to (4.2). It can be seen that  $\langle \hat{\phi}_{\mathbf{m}}^{x,0} \rangle$  tends toward smaller values as the lattice regulator is removed, contrary to the classical expectations (3.20). At large enough values of  $N$  the curves flatten out to a constant value.

To understand this behavior, we first note that we are computing an expectation value that is already nonvanishing in the undeformed theory ( $\mu \equiv 0$ ). The undeformed theory expectation values

$$\langle g^{-1} \phi_{\mathbf{m}}^{x,0} \rangle = \langle \hat{g}^{-1} \hat{\phi}_{\mathbf{m}}^{x,0} \rangle \quad (4.4)$$

for various values of  $N$  are shown in Fig. 2. The rescaling by  $g^{-1} = a^2 \hat{g}^{-1}$  is useful because it corresponds to removing  $g$  from the undeformed action  $S_0$  by a rescaling of the lattice variables [cf. (2.1)]; this amounts to studying the undeformed theory in units of  $\sqrt{g}$ . It can be seen from Fig. 2 that (4.4) is far from zero, and is rather insensitive to  $N$ . The undeformed theory only contains two length scales,  $1/\sqrt{g}$  and  $N/\sqrt{g}$ . For large  $N$ , it is not surprising that the *local* expectation value (4.4) is insensitive to the long distance scale  $N/\sqrt{g}$ . Rather, it is determined by the short distance scale  $1/\sqrt{g}$ . The deformed theory retains this short distance scale. Once the system size is much larger than this scale, the local expectation value becomes independent of the system volume; this is particularly true because the relative strength of the deformation is being scaled to zero [cf. (4.3)].

In Table 1 we show the large  $N$  expectation values (4.4) in the deformed theory as well as those of the undeformed theory. Here, the values for  $N = 16, 18, 20$  were averaged for each  $\hat{g}^{-1}$ , which should provide a good estimate of the asymptotic value, as can be seen in Fig. 1. The error was estimated based on the maximum deviation from this mean, among the three data points, taking into account the  $1\sigma$  error estimates that have been represented in the figure by error bars. Table 1 shows that the large  $N$  expectation values (4.4) *in the deformed theory* are (up to statistical errors) the same as those of the *undeformed theory*.

Incidentally, one might worry that due to the nontrivial moduli space of the undeformed theory, its partition function (for the purely bosonic theory) is not well-defined. Certainly this is the case for the 0d reduction of  $d \leq 4$   $SU(2)$  pure Yang-Mills; however, this is not the case—in spite of noncompact flat directions—for the 0d reduction of  $d \geq 5$   $SU(2)$  pure Yang-Mills; see Eq. (24) of [12]. This is because, properly speaking, the classical moduli space is a set of measure zero in the field integration of the partition function. For  $d \geq 5$ , “entropic effects of the measure...overwhelm the possible divergences” [12]. We are not aware of any exact result showing that the partition function of the CKKU quiver system obtained

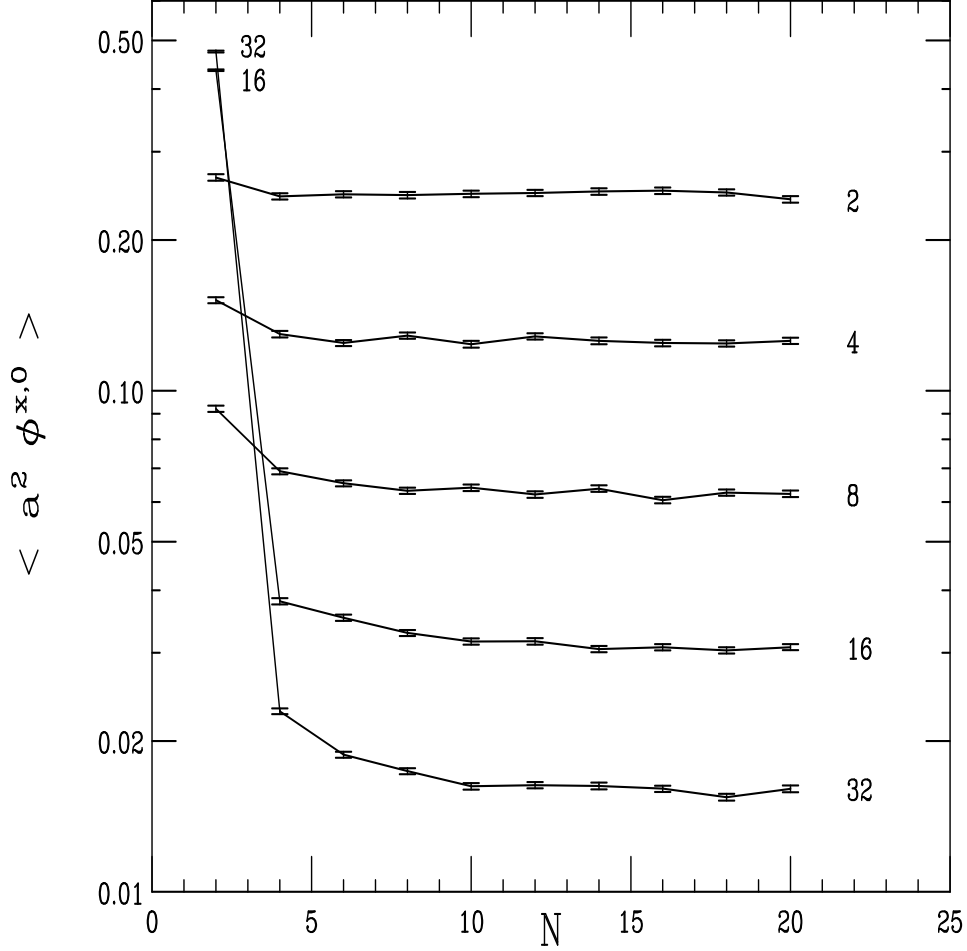


Figure 1: Trajectories of fixed lattice spacing, increasing volume, with data connected by lines to guide the eye. Each line is marked by the corresponding value of  $\hat{g}^{-1}$ . A doubling of  $\hat{g}^{-1}$  corresponds to a halving of the lattice spacing.

$\hat{g}^{-1}$	$\langle \hat{\phi}^{x,0} \rangle$	$\langle \hat{g}^{-1} \hat{\phi}^{x,0} \rangle$
2	0.2469(94)	0.494(19)
4	0.1249(27)	0.500(11)
8	0.0618(22)	0.494(18)
16	0.03064(75)	0.490(12)
32	0.01586(64)	0.507(21)
1 ( $\mu \equiv 0$ )		0.496(22)

Table 1: Large  $N$  asymptotic values for the  $\hat{\mu}^{-1} = N$  trajectories. For comparison, the result for the undeformed ( $\mu \equiv 0$ ) expectation value is shown in the bottom line. Estimated errors in the last 2 digits are shown in parentheses.

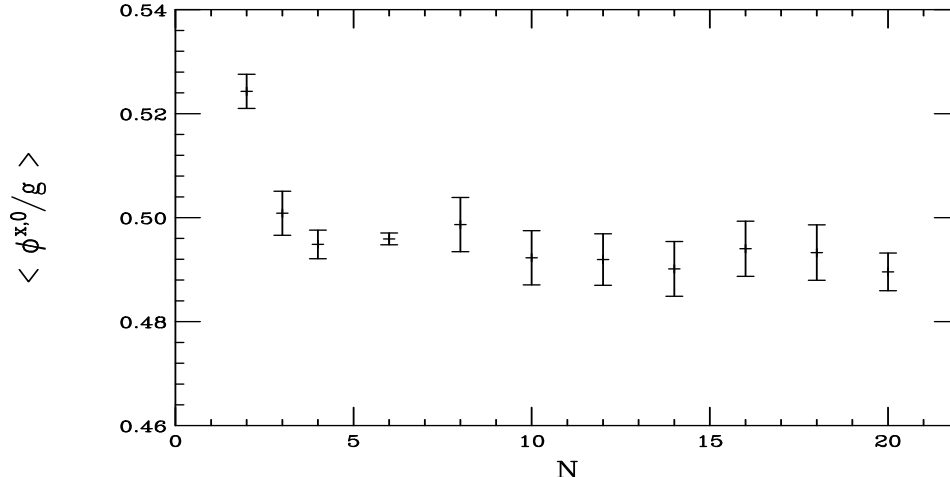


Figure 2: Undeformed theory results. Error bars differ in size due to differing numbers of samples.

from the  $6d \rightarrow 0d$   $SU(kN^2)$  pure Yang-Mills is divergent.<sup>4</sup> In our view it is unlikely, just from the result that  $6d \rightarrow 0d$   $SU(2)$  pure Yang-Mills has a finite partition function. Furthermore, if there was a problem with the partition function of the undeformed theory, we would have expected an uncontrolled dispersion in our observables when we attempted to measure them in the undeformed theory. This is because flat directions not suppressed by entropic effects would allow for the Monte Carlo simulation to wander wildly throughout configuration space, leading to results that would not converge to reliable average values. That this did not occur is further evidence that the partition function is well-defined. Finally, the deformation  $S_{SB}$  can be regarded as a regulator of any possible divergence associated with the noncompact flat directions. That we obtain stable, identical results as the deformation is removed provides further evidence that our expectation values for the undeformed theory are reliable.

## 5 Interpretation

In our simulations of the purely bosonic system, we have observed that under the scaling (4.3), the deformation becomes ineffective at changing the expectation value (4.4), or equivalently (4.1), away from the value that would be obtained in the undeformed theory. What has happened is that the flat directions that were lifted by the deformation are becoming flat all over again as  $N \rightarrow \infty$ . More precisely, the deformation is proportional to  $1/g_2^2 L^2$ , and in the thermodynamic limit this quantity vanishes. Whereas the configurations of the moduli space of the undeformed theory that were lifted by  $S_{SB}$  cost energy at finite  $N$ , the number of such configurations is becoming vast due to the approximate flatness in those directions.

<sup>4</sup>The diagonal  $U(1)$  from  $U(kN^2) = U(1) \times SU(kN^2)$  decouples; its (divergent) contribution to the partition function trivially factors out.

For  $N \gtrsim \hat{g}^{-1/2}$ , the entropy of these configurations wins out over the energy arguments that prefer (3.20).

One lifted region of the  $S_0$  moduli space where this is particularly clear is the branch (3.6). The action for such configurations is (setting  $c = 1$ )

$$S_B = \frac{1}{2\hat{g}^2} + \frac{2}{\hat{g}^2 N^2} \sum_{\mathbf{m}} (|\hat{z}_{\mathbf{m}}^0|^2 + |\hat{z}_{\mathbf{m}}^3|^2) = \frac{N^2}{2g_2^2 L^2} + \frac{2}{g_2^2 L^2} \sum_{\mathbf{m}} (|\hat{z}_{\mathbf{m}}^0|^2 + |\hat{z}_{\mathbf{m}}^3|^2) \quad (5.1)$$

Integrating  $\exp(-S_B)$  over all  $\hat{z}_{\mathbf{m}}^{0,3}$  we obtain

$$\left(\frac{\pi}{2}\right)^{2N^2} \exp\left[\frac{N^2}{2g_2^2 L^2} (-1 + 4g_2^2 L^2 \ln(g_2^2 L^2))\right] \quad (5.2)$$

Note that for large system size  $g_2 L \gg 1$ . Thus, the positive (entropic) term under the exponential wins out over the negative (energetic) term by a large margin. It would seem that the weight of these configurations increases exponentially as we increase  $N$  while holding  $g_2 L$  fixed; that is, in the continuum limit.

Indeed the observed behavior summarized in Table 1 is that in the deformed theory

$$\left\langle \frac{1}{2} \text{Tr} (\hat{x}_{\mathbf{m}} \hat{x}_{\mathbf{m}}^\dagger) \right\rangle \approx \frac{g_2 L}{2N} = \frac{1}{2} g_2 a \quad (5.3)$$

Thus the simulations likewise indicate that configurations with  $\hat{x}_{\mathbf{m}} = 0$  are dominating as we increase  $N$  while holding  $g_2 L$  fixed, which is nothing but the continuum limit. By symmetry, the same also holds for  $\hat{y}_{\mathbf{m}}$ .

## 6 Including fermions

While the above results and arguments for the non-supersymmetric system are interesting in their own right, it is essential to include the fermions if we are to draw conclusions for the supersymmetric system.

Unfortunately, the present system suffers from a complex fermion determinant [2]. Thus the integration measure  $\det M e^{-S_B}$  is not positive semi-definite and does not provide a satisfactory probability measure for Monte Carlo simulations. If we factor out the phase  $e^{i\alpha} = \det M / |\det M|$  and use  $|\det M| e^{-S_B}$  instead, then we will generate the *phase-quenched* (*p.q.*) ensemble of boson configurations. Expectation values of an operator  $\mathcal{O}$  in the full theory are formally related to those in the phase-quenched theory by the *reweighting* identity

$$\langle \mathcal{O} \rangle = \langle e^{i\alpha} \mathcal{O} \rangle_{p.q.} / \langle e^{i\alpha} \rangle_{p.q.} \quad (6.1)$$

In some lattice systems, the distribution of  $\alpha$  in the phase-quenched ensemble is sharply peaked. The phase-quenched quantities in the ratio exist and can be measured reliably. For example, this is the case in the 4d  $U(1)_L \times U(1)_R$  symmetric Yukawa model of [13]. By

contrast, the results of [2] for the CKKU system are not encouraging. The distribution of  $\alpha$  (denoted  $\phi$  in that work) in the phase-quenched ensemble was found to be essentially flat. This leads to approximate cancellations when we attempt to compute reweighted quantities contained in the numerator and denominator of (6.1). More details will be given below. Here we merely emphasize that we do not expect the strategy implied by (6.1) to succeed, in practice, for the present system. Our chief result will thus be to quantify the degree to which it fails.

As will be seen below in Sec. 6.2,  $\det M$  vanishes for the  $S_0 = 0$  configurations that were discussed above. Thus the configurations that have the most weight in the fully-quenched ensemble are configurations that have vanishing weight in the phase-quenched ensemble. (Further quantification of this statement is given in Sec. 6.3.) For this reason we find it interesting to study the quantity  $\langle \hat{\phi}_{\mathbf{m}}^{x,0} \rangle_{p,q}$ , in Sec. 6.4. Certainly this bears a closer resemblance to the expectation value in the full theory, in that the suppression due to very small  $|\det M|$  is taken into account for configurations in the neighborhood of the undeformed moduli space. In Sec. 6.5, we return to the matter of phase reweighting.

## 6.1 Fermion action

First we review the fermion action in the notation of [2]. The fermion action can be written in the form

$$S_F = -\frac{1}{g^2} (\psi_{1,\mathbf{m}}^\mu, \psi_{2,\mathbf{m}}^\mu, \psi_{3,\mathbf{m}}^\mu, \chi_{\mathbf{m}}^\mu) \cdot M_{\mathbf{m}\mathbf{n}}^{\mu\rho} \cdot \begin{pmatrix} \xi_{1,\mathbf{n}}^\rho \\ \xi_{2,\mathbf{n}}^\rho \\ \xi_{3,\mathbf{n}}^\rho \\ \lambda_{\mathbf{n}}^\rho \end{pmatrix} \quad (6.2)$$

The elements of the fermion matrix are:

$$\begin{aligned} (M_{\mathbf{m}\mathbf{n}}^{\mu\rho})_{1,1} &= (M_{\mathbf{m}\mathbf{n}}^{\mu\rho})_{2,2} = (M_{\mathbf{m}\mathbf{n}}^{\mu\rho})_{3,3} = (M_{\mathbf{m}\mathbf{n}}^{\mu\rho})_{4,4} = 0, \\ (M_{\mathbf{m}\mathbf{n}}^{\mu\rho})_{1,2} &= -t_{\mathbf{m},\mathbf{n}}^{\mu\nu\rho} z_{\mathbf{n}+\hat{i}}^\nu + t_{\mathbf{m},\mathbf{n}}^{\mu\rho\nu} z_{\mathbf{n}}^\nu, & (M_{\mathbf{m}\mathbf{n}}^{\mu\rho})_{1,3} &= t_{\mathbf{m},\mathbf{n}}^{\mu\nu\rho} y_{\mathbf{n}+\hat{i}}^\nu - t_{\mathbf{m},\mathbf{n}+\hat{j}}^{\mu\rho\nu} y_{\mathbf{n}}^\nu, \\ (M_{\mathbf{m}\mathbf{n}}^{\mu\rho})_{1,4} &= t_{\mathbf{m},\mathbf{n}}^{\mu\nu\rho} \bar{x}_{\mathbf{n}}^\nu - t_{\mathbf{m},\mathbf{n}-\hat{i}}^{\mu\rho\nu} \bar{x}_{\mathbf{m}}^\nu, & (M_{\mathbf{m}\mathbf{n}}^{\mu\rho})_{2,1} &= t_{\mathbf{m},\mathbf{n}}^{\mu\nu\rho} z_{\mathbf{n}+\hat{j}}^\nu - t_{\mathbf{m},\mathbf{n}}^{\mu\rho\nu} z_{\mathbf{n}}^\nu, \\ (M_{\mathbf{m}\mathbf{n}}^{\mu\rho})_{2,3} &= -t_{\mathbf{m},\mathbf{n}}^{\mu\nu\rho} x_{\mathbf{n}+\hat{j}}^\nu + t_{\mathbf{m},\mathbf{n}+\hat{i}}^{\mu\rho\nu} x_{\mathbf{n}}^\nu, & (M_{\mathbf{m}\mathbf{n}}^{\mu\rho})_{2,4} &= t_{\mathbf{m},\mathbf{n}}^{\mu\nu\rho} \bar{y}_{\mathbf{n}}^\nu - t_{\mathbf{m},\mathbf{n}-\hat{j}}^{\mu\rho\nu} \bar{y}_{\mathbf{m}}^\nu, \\ (M_{\mathbf{m}\mathbf{n}}^{\mu\rho})_{3,1} &= -t_{\mathbf{m},\mathbf{n}}^{\mu\nu\rho} y_{\mathbf{n}}^\nu + t_{\mathbf{m},\mathbf{n}+\hat{j}}^{\mu\rho\nu} y_{\mathbf{n}}^\nu, & (M_{\mathbf{m}\mathbf{n}}^{\mu\rho})_{3,2} &= t_{\mathbf{m},\mathbf{n}}^{\mu\nu\rho} x_{\mathbf{n}}^\nu - t_{\mathbf{m},\mathbf{n}+\hat{i}}^{\mu\rho\nu} x_{\mathbf{n}}^\nu, \\ (M_{\mathbf{m}\mathbf{n}}^{\mu\rho})_{3,4} &= t_{\mathbf{m},\mathbf{n}}^{\mu\nu\rho} \bar{z}_{\mathbf{n}}^\nu - t_{\mathbf{m},\mathbf{n}}^{\mu\rho\nu} \bar{z}_{\mathbf{n}}^\nu, & (M_{\mathbf{m}\mathbf{n}}^{\mu\rho})_{4,1} &= -t_{\mathbf{m},\mathbf{n}}^{\mu\nu\rho} \bar{x}_{\mathbf{n}+\hat{j}}^\nu + t_{\mathbf{m},\mathbf{n}-\hat{i}}^{\mu\rho\nu} \bar{x}_{\mathbf{m}}^\nu, \\ (M_{\mathbf{m}\mathbf{n}}^{\mu\rho})_{4,2} &= -t_{\mathbf{m},\mathbf{n}}^{\mu\nu\rho} \bar{y}_{\mathbf{n}+\hat{i}}^\nu + t_{\mathbf{m},\mathbf{n}-\hat{j}}^{\mu\rho\nu} \bar{y}_{\mathbf{m}}^\nu, & (M_{\mathbf{m}\mathbf{n}}^{\mu\rho})_{4,3} &= -t_{\mathbf{m},\mathbf{n}}^{\mu\nu\rho} \bar{z}_{\mathbf{n}+\hat{i}+\hat{j}}^\nu + t_{\mathbf{m},\mathbf{n}}^{\mu\rho\nu} \bar{z}_{\mathbf{n}}^\nu. \end{aligned} \quad (6.3)$$

$$\begin{aligned} T^\mu &= (\mathbf{1}_2, \sigma^a), & \text{Tr}(T^\mu T^\nu T^\rho) &= 2t^{\mu\nu\rho} & \Rightarrow \\ t^{000} &= 1, & t^{a00} &= 0, & t^{ab0} &= \delta^{ab}, & t^{abc} &= i\epsilon^{abc} \\ t_{\mathbf{m},\mathbf{n}}^{\mu\nu\rho} &= \delta_{\mathbf{m},\mathbf{n}} t^{\mu\nu\rho} \end{aligned} \quad (6.4)$$

This matrix has two ever-present fermion zeromodes. The first is associated with left multiplication (the transpose ‘‘T’’ merely indicates a row vector, for consistency with (6.2)):

$$(\xi_{1,\mathbf{n}}^\rho, \xi_{2,\mathbf{n}}^\rho, \xi_{3,\mathbf{n}}^\rho, \lambda_{\mathbf{n}}^\rho)^T = (0, 0, 0, \lambda\delta^{\rho 0})^T \quad \forall \quad \mathbf{n} \quad (6.5)$$

The second is associated with right multiplication:

$$(\psi_{1,\mathbf{m}}^\mu, \psi_{2,\mathbf{m}}^\mu, \psi_{3,\mathbf{m}}^\mu, \chi_{\mathbf{m}}^\mu) = (0, 0, \psi\delta^{0\mu}, 0) \quad \forall \mathbf{m} \quad (6.6)$$

Because the matrix  $M$  is not hermitian, it is diagonalized by  $M \rightarrow D = U M V$  with  $U$  and  $V$  independent unitary matrices. When this is done, the diagonal matrix  $D$  always has 2 zeros on the diagonal, one each from (6.5) and (6.6).

The zeromode eigenvalues of the daughter theory can be factored out following the method used in [2, 3]. We deform the fermion matrix appearing in (6.2) according to

$$M \rightarrow M_\epsilon \equiv M + \epsilon \mathbf{1}_{N_f} \quad (6.7)$$

where  $N_f = 16N^2$  is the dimensionality of the fermion matrix and  $\epsilon \ll 1$  is a deformation parameter that we will eventually take to zero. We factor out the zero mode through the definition

$$\hat{M}_0 = \lim_{\epsilon \rightarrow 0^+} \hat{M}_\epsilon, \quad \hat{M}_\epsilon \equiv \epsilon^{-2/N_f} M_\epsilon \Rightarrow \det \hat{M}_0 = \lim_{\epsilon \rightarrow 0^+} \epsilon^{-2} \det M_\epsilon. \quad (6.8)$$

If this deformation is added to the action, it explicitly breaks the exact lattice supersymmetry and gauge invariance. This infrared regulator could be removed in the continuum limit, say, by taking  $\epsilon a \ll N^{-1}$ . Noting that  $L = Na$  is the physical size of the lattice, the equivalent requirement is that  $\epsilon \ll L^{-1}$  be maintained as  $a \rightarrow 0$ , for fixed  $L$ . Thus in the thermodynamic limit ( $L \rightarrow \infty$ ), the deformation is removed. The parameter  $\epsilon$  is a soft infrared regulating mass, and is quite analogous to the soft mass  $\mu$  introduced by CKKU [1] in their Eq. (1.2) to control the bosonic zeromode of the theory. In the same way that the deformation introduced with  $\mu$  does not modify the final results of the renormalization analysis of Section 3.4 of [1], our  $\epsilon$  does not modify the result of the quantum continuum limit. The essence of the argument is that we have introduced a vertex that will be proportional to the dimensionless quantity  $g_2^2 \epsilon a^3 \ll g_2^2 a^3 / L$ , where  $g_2$  is the 2d coupling constant. Such contributions to the operator coefficients  $C, \hat{C}$  in Eq. (3.29) of [1] vanish in the thermodynamic limit. Because the target theory is super-renormalizable, we are assured that the perturbative power counting arguments are reliable and the correct continuum limit is obtained.

In [2], we studied the convergence of  $\det \hat{M}_\epsilon \rightarrow \det \hat{M}_0$ . We found that the convergence was rapid and that a reliable estimate for  $\det \hat{M}_0$  can be obtained in this way. As a check, we computed the eigenvalues of the undeformed matrix  $M$ , using the math package Maple, for 10 random boson configurations. We found that the product of nonzero eigenvalues agreed with  $\det \hat{M}_0$  in magnitude and phase to within at least 5 significant digits.

In the phase-quenched ensemble, we take the probability measure defined by  $|\det M_\epsilon| e^{-S_B}$ , with  $\epsilon = 10^{-6}$ . Our numerical studies indicate that this  $\epsilon$  is more than small enough to factor out the ever-present zeros while leaving the nonzero eigenvalues virtually unchanged. We have dropped the factor of  $\epsilon^{-2}$  that distinguishes between  $\hat{M}_\epsilon$  and  $M_\epsilon$ . This is permissible because it cancels in correlation functions. In the simulation, this is reflected in the fact that under a shift in the boson configuration,  $\delta \ln |\det \hat{M}_\epsilon| = \delta \ln |\det M_\epsilon|$ , since  $-2 \ln \epsilon$  is



a constant. The value  $\epsilon = 10^{-6}$  renders  $M_\epsilon$  rather ill-conditioned, so we must use a very accurate inversion algorithm (see below). As an aside, we have found that approximation of  $M_\epsilon^{-1}$  by noisy estimators fails because the biconjugate gradient algorithm cannot handle the ill-conditioned matrix. This is the main obstacle that we have faced in our attempts to extend our analysis beyond  $N = 6$ . Note that for  $N = 6$ , the matrix  $M_\epsilon$  is already  $576 \times 576$  with complex entries.

## 6.2 Determinant on moduli space

We have stated above that the effects of fermions must be taken into account in order to draw conclusions about observables of the supersymmetric system. One way to see this is to consider the fermion determinant in the case where we set the boson configuration to one of the points of the undeformed theory moduli space discussed above in Sec. 3.1. We now show that additional fermion zeromodes appear in these boson configurations. This seems reasonable if we regard the lattice action as the Hamiltonian of a classical statistical system. Zero action boson configurations correspond to bosons of zero energy. By the exact supersymmetry of the undeformed system, we expect that these zero energy bosonic states have fermionic partners, also of zero energy. These fermion zeromodes will cause the fermion matrix to be more singular.<sup>5</sup> Indeed, this heuristic argument seems borne out by the examples below. However, we were unable to construct an explicit proof; presumably it would involve a study of eigenvalues of the transfer matrix corresponding to the lattice action.

### 6.2.1 $x_{\mathbf{m}} = y_{\mathbf{m}} = 0$ non-zeromode branch

Here we can choose

$$(\xi_{1,\mathbf{n}}^\rho, \xi_{2,\mathbf{n}}^\rho, \xi_{3,\mathbf{n}}^\rho, \lambda_{\mathbf{n}}^\rho)^T = (0, 0, 0, \lambda_{\mathbf{n}} \delta^{\rho 0})^T \quad (6.9)$$

It is easily checked that  $M$  acting on this vector vanishes for any choice of the  $N^2$  Grassmann variables  $\lambda_{\mathbf{n}}$ . This gives  $N^2$  fermion zeromodes associated with left multiplication. We also have  $N^2$  fermion zeromodes associated with right multiplication:

$$(\psi_{1,\mathbf{m}}^\mu, \psi_{2,\mathbf{m}}^\mu, \psi_{3,\mathbf{m}}^\mu, \chi_{\mathbf{m}}^\mu) = (0, 0, \psi_{\mathbf{m}} \delta^{0\mu}, 0) \quad (6.10)$$

Note that the number of zeromodes,  $2N^2$ , is the same as the number of (complex) boson zeromodes found in Sec. 3.1.2 above.

Two of these modes are the ever-present zeromodes discussed in Sec. 6.1 above. The other  $2(N^2 - 1)$  are zeros special to this branch of moduli space. Strictly speaking, the set of configurations that satisfy  $x_{\mathbf{m}} = y_{\mathbf{m}} = 0$  is a set of measure zero in the lattice partition function. But taking a small neighborhood of radius  $\delta$  about this subspace—that is, small fluctuations about the classical configuration—we see that  $\det M_\epsilon \propto \epsilon^2 \delta^{2(N^2-1)}$  in this region,

---

<sup>5</sup>These observations were pointed out to us by a referee of an earlier version of this report [14].

where the powers of  $\delta$  come from the  $2(N^2 - 1)$  fermion approximately-zero-modes that are present near the  $x_{\mathbf{m}} = y_{\mathbf{m}} = 0$  branch. Thus the inclusion of fermions dramatically changes the weight of configuration space in the neighborhood of  $x_{\mathbf{m}} = y_{\mathbf{m}} = 0$  branch in the integration measure; it has become totally negligible. Thus *we do not expect the entropic effects discussed in Sec. 5 to persist in the supersymmetric system*. As a consequence, we expect to get a very different value for  $\langle \phi^{x,0} \rangle$ .

### 6.2.2 $z_{\mathbf{m}} = 0$ non-zeromode branch

First consider the case where  $\omega^{k'_1+k'_2} = 1$ . Then set

$$(\xi_{1,\mathbf{n}}^\rho, \xi_{2,\mathbf{n}}^\rho, \xi_{3,\mathbf{n}}^\rho, \lambda_{\mathbf{n}}^\rho)^T = (0, 0, \delta^{\rho 0} \xi, 0)^T \quad \forall \quad \mathbf{n} \quad (6.11)$$

It is easy to check that this is a fermion zeromode on this branch, for any choice of  $\xi$ . There is also a corresponding fermion zeromode of right multiplication:

$$(\psi_{1,\mathbf{m}}^\mu, \psi_{2,\mathbf{m}}^\mu, \psi_{3,\mathbf{m}}^\mu, \chi_{\mathbf{m}}^\mu) = (0, 0, 0, \delta^{\mu 0} \chi) \quad \forall \quad \mathbf{m} \quad (6.12)$$

Now consider the case where  $\omega^{k'_1+k'_2} = -1$ . Then set

$$(\xi_{1,\mathbf{n}}^\rho, \xi_{2,\mathbf{n}}^\rho, \xi_{3,\mathbf{n}}^\rho, \lambda_{\mathbf{n}}^\rho)^T = (0, 0, \delta^{\rho 0} (-)^{n_1+n_2} \xi, 0)^T \quad \forall \quad \mathbf{n} \quad (6.13)$$

It is only slightly more work to check that this is a fermion zeromode on this branch. There is also a corresponding fermion zeromode of right multiplication:

$$(\psi_{1,\mathbf{m}}^\mu, \psi_{2,\mathbf{m}}^\mu, \psi_{3,\mathbf{m}}^\mu, \chi_{\mathbf{m}}^\mu) = (0, 0, 0, \delta^{\mu 0} (-)^{m_1+m_2} \chi) \quad \forall \quad \mathbf{m} \quad (6.14)$$

We note that the suppression due to the fermion determinant is much smaller, relative to the  $x_{\mathbf{m}} = y_{\mathbf{m}} = 0$  branch, in the neighborhood of this branch:  $\det M_\epsilon \propto \epsilon^2 \delta^2$ .

## 6.3 Determinant distribution in the fully-quenched ensemble

Formally, the expectation value of an operator  $\mathcal{O}$  in the phase-quenched ensemble is related to a ratio of expectation values in the fully-quenched (*f.q.*) ensemble:

$$\langle \mathcal{O} \rangle_{p.q.} = \langle |\det M| \mathcal{O} \rangle_{f.q.} / \langle |\det M| \rangle_{f.q.} \quad (6.15)$$

This is a type of reweighting identity. However, for this to work in practice, it is necessary that there be a significant overlap between the phase-quenched ensemble and the fully-quenched ensemble. We now show that this is certainly not the case in the present system, which is just to say that the fully-quenched expectation values have no bearing on the system with fermions. Our main point here is just to show that the inclusion of the effects of fermions *in the updating process of the Monte Carlo simulation* is crucial to the study of the supersymmetric system, a not very surprising result. We now quantify this statement by an analysis of the impracticality of (6.15).

We accumulate  $N_s$  points of data in the fully-quenched ensemble and then bin them according to  $\ln |\det M|$ . From the number of samples  $n_i$  in each bin  $i$ , we obtain an estimate  $w_i \approx n_i/N_s$  of the weight of each bin. We denote the average value of  $\phi_{\mathbf{m}}^{x,0}$  in each bin by  $\langle \phi_{\mathbf{m}}^{x,0} \rangle_i$ . We denote

$$|\det M|_i = \exp(\text{central value of } \ln |\det M| \text{ in bin } i) \quad (6.16)$$

In principal, as the number of bins is taken to infinity and the resolution of each bin is taken to be infinitely fine, the approximations

$$\begin{aligned} \langle |\det M| \phi_{\mathbf{m}}^{x,0} \rangle_{f.q.} &\approx \sum_i w_i |\det M|_i \langle \phi_{\mathbf{m}}^{x,0} \rangle_i \\ \langle |\det M| \rangle_{f.q.} &\approx \sum_i w_i |\det M|_i \end{aligned} \quad (6.17)$$

become exact. In practice, however, we always have truncation errors from using a finite number of bins, and systematic errors from finite resolution. Furthermore, the statistics in all of the bins that contribute significantly to these sums must be large, so that error estimates for the quantities  $w_i$  and  $\langle \phi_{\mathbf{m}}^{x,0} \rangle_i$  are reasonably small.

In Fig. 3 we show  $w_i$ ,  $\langle \phi_{\mathbf{m}}^{x,0} \rangle_i$  and  $w_i |\det M|_i$  as a function of  $\log_{10} |\det M|_i$ . It can be seen that the overall weight  $w_i |\det M|_i$  is sharply peaked in a region where  $w_i$  is very small. (On the plot,  $w_i$  is indistinguishable from zero in this region; numerically, it is  $\mathcal{O}(10^{-4})$ .) The estimate of  $\langle \phi_{\mathbf{m}}^{x,0} \rangle_i$  in these upper bins is very inaccurate, due to a small number of samples. In fact, even for 10000 samples, we were not able to see the right-hand side of the peak! Thus it is impossible to estimate the truncation error that results from having data for only a finite number of bins. For the present system, it is not possible to get a reliable estimate of either of the averages on the right-hand side of (6.15). This is consistent with the results of Sec. 6.2: the fully-quenched ensemble gives its largest weight to configurations that have practically no weight in the phase-quenched ensemble. Thus the overlap is essentially nil, rendering (6.15) quite useless. Another conclusion that we can draw from this is: expectation values obtained in the fully-quenched ensemble are not a good indicator, to any degree of approximation, of expectation values that would be obtained in the phase-quenched ensemble.

## 6.4 Results for the phase-quenched ensemble

In Fig. 4  $\langle \hat{\phi}_{\mathbf{m}}^{x,0} \rangle$  is obtained in the phase-quenched ensemble; that is, the fermion determinant was taken into account in Metropolis updates, using the linear variation

$$\delta \ln |\det M_\epsilon| = \text{Re Tr} [M_\epsilon^{-1} \delta M_\epsilon] \quad (6.18)$$

As usual, we worked at  $\epsilon = 10^{-6}$ , so that the ever-present fermion zeromodes factor out. This renders  $M_\epsilon$  ill-conditioned. To invert the matrix reliably, we have used triangular (LU) decomposition by Crout's method, which is very accurate. We have checked that the inversion is good to 1 part in  $10^6$  in our simulations.

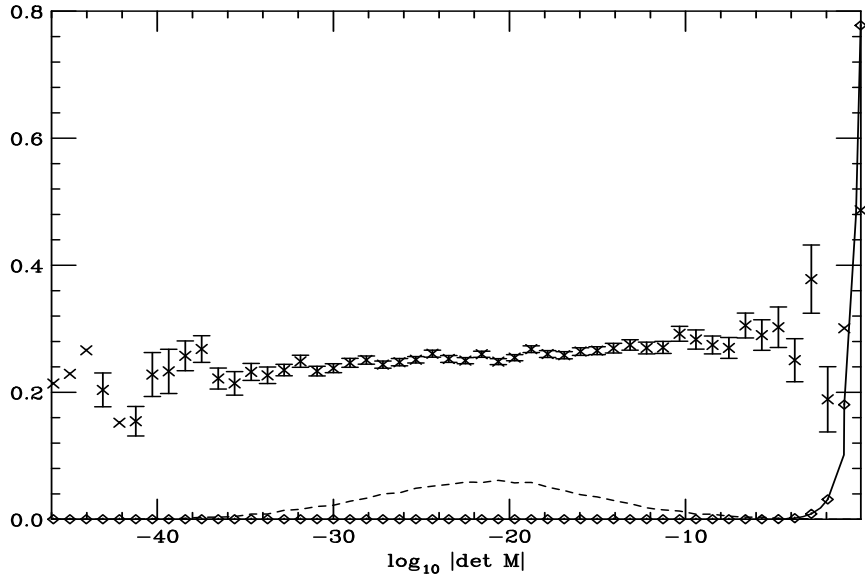


Figure 3: The dashed line is  $w_i$ . The solid line connects data for  $w_i |\det M|_i$ , marked by diamonds. Data marked by an “x” represent  $\langle \phi_{\mathbf{m}}^{x,0} \rangle_i$ . Where error bars are not shown for the  $\langle \phi_{\mathbf{m}}^{x,0} \rangle_i$  data, only 1 or 2 points of data were available, so no estimate of error could be made. This plot is for 10000 samples on a  $6 \times 6$  lattice with  $\hat{g}^{-1} = 2$ .

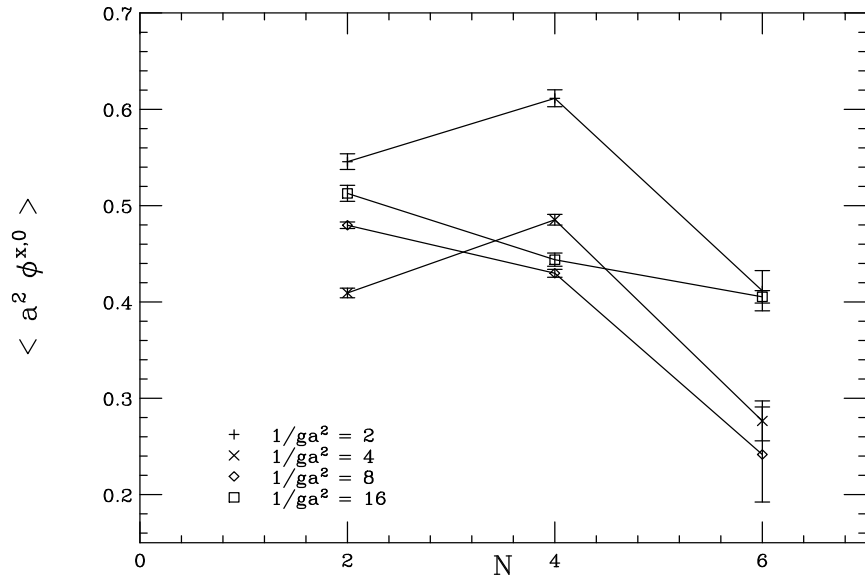


Figure 4: Phase-quenched averages (lines to guide the eye).

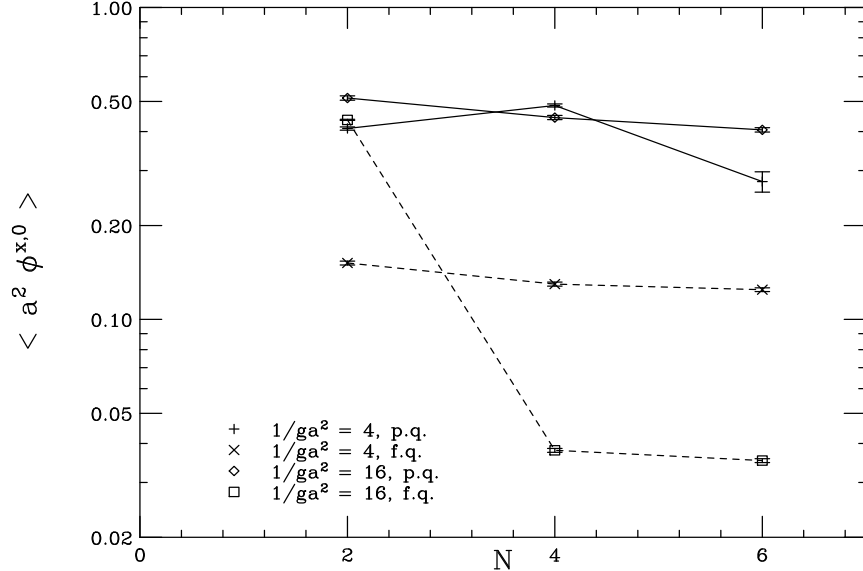


Figure 5: A comparison of some of the averages obtained in phase-quenched (solid lines to guide the eye) versus fully-quenched (dashed lines to guide the eye) simulations.

We remind the reader that larger values of  $\hat{g}^{-1} = 1/ga^2$  correspond to finer lattices, and thus extrapolate to the continuum limit. However, to hold  $L = Na$  fixed, successive trajectories must be compared as  $N$  versus  $2N$ , since  $\hat{g}^{-1}$  is doubled. It can be seen from Fig. 4 that for  $N \leq 6$  it is not possible to extrapolate to the large  $L$  behavior. The best we can say is the following. In Fig. 5 we provide a comparison between the phase-quenched and fully-quenched results. It can be seen that the effect of the fermion determinant is dramatic. For the finest lattice that we have available,  $\hat{g}^{-1} = 16$ , the phase-quenched results are more than an order of magnitude larger when we look at  $N = 6$ . Furthermore, the phase-quenched results are always of the same order of magnitude as the classical estimate (3.20).

## 6.5 Phase reweighting

As has been reported earlier [2], and mentioned above, the distribution of  $\alpha = \arg \det \hat{M}_0$  is essentially flat with respect to the phase-quenched ensemble. In Fig. 6 we present results for a  $2 \times 2$  lattice. It can be seen that it will be quite difficult to obtain a reliable estimate of  $\langle \exp(i\alpha) \rangle_{p.q.}$ .

E.g., we find that for  $N = 2$ ,  $\hat{g}^{-1} = 2$ , with 1000 samples, the “noise-to-signal” ratio is

$$\sigma_{\langle \cos \alpha \rangle_{p.q.}} / \langle \cos \alpha \rangle_{p.q.} = \sigma_{\langle \sin \alpha \rangle_{p.q.}} / \langle \sin \alpha \rangle_{p.q.} = \mathcal{O}(1) \quad (6.19)$$

For  $N = 4$ ,  $\hat{g}^{-1} = 2$ , with 1000 samples, we find

$$\sigma_{\langle \cos \alpha \rangle_{p.q.}} / \langle \cos \alpha \rangle_{p.q.} = \sigma_{\langle \sin \alpha \rangle_{p.q.}} / \langle \sin \alpha \rangle_{p.q.} = \mathcal{O}(10) \quad (6.20)$$

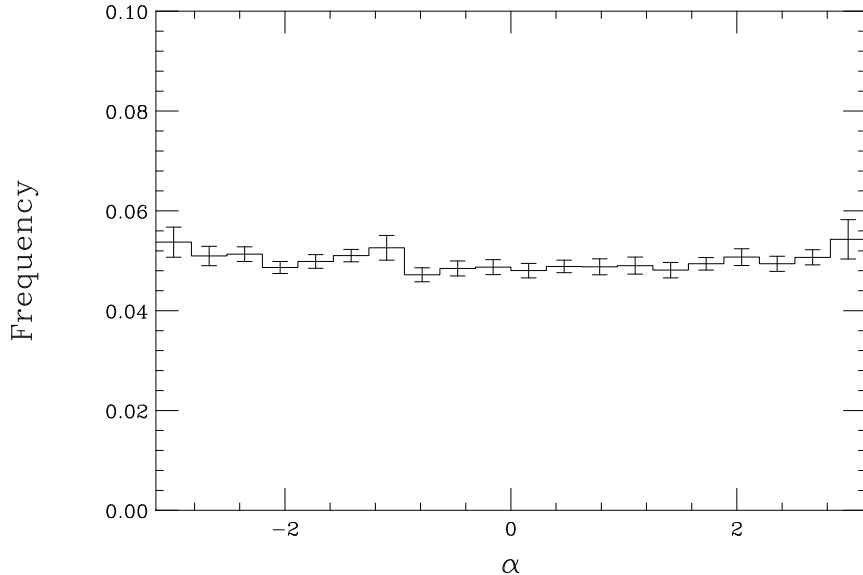


Figure 6: Average frequency distribution for  $\alpha = \arg \det \hat{M}_0$  in the phase-quenched distribution for the  $2 \times 2$  lattice. Error bars are determined by variance in bin counts for several blocks of data.

On general grounds, these noise-to-signal ratios are expected to get exponentially worse as  $N$  is increased. Similarly discouraging results are found for the other quantities that need to be estimated in order to make use of the reweighting identity (6.1). Since reweighting does not even work for small  $N$ , it looks like a futile approach by which to study the full theory.

## 7 Conclusions

In the fully-quenched system we have found that the classical estimate for the expectation value  $\langle \phi^{x,0} \rangle$  is not reliable. We have argued that this is due to entropic effects that dominate when the relative strength of the deformation is scaled to zero. Thus we conclude that the fully-quenched system does not yield the nonsupersymmetric gauge theory in the quantum continuum limit. However, we regard it as an interesting question whether or not a well-defined continuum theory is obtained if the relative strength of the deformation is not scaled to zero. We have not investigated this question as it is beyond the intended scope of this article.

Next we have shown that the fermion determinant tends to vanish in the neighborhood of the configurations that were argued to yield the dominating entropic effects. It follows that the fully-quenched ensemble will not provide a reliable guide to the physics of the full, supersymmetric theory. We have studied  $\langle \phi^{x,0} \rangle$  in the phase-quenched ensemble. We have found a dramatic increase in the expectation value that is obtained. We regard this as encouraging for the CKKU proposal.

However, to truly obtain data on the full lattice theory proposed by CKKU, it is necessary to take into account the complex phase of the fermion determinant. We have discussed the notion of reweighting by the phase of the determinant. However, we know from previous work that the distribution of this phase in the phase-quenched ensemble is so nearly flat that it is not practical to obtain reweighted quantities. As a practical matter, it seems impossible to study the continuum limit of the full theory by Monte Carlo methods, unless there is significant progress in the technique for the treatment of the complex phase of the fermion determinant.

In this regard, we remark that the complex phase is not present in the target continuum theory; so, it may be possible to address the phase by blocking out the short distance modes of the lattice theory. However, this too is beyond the scope of this report. Alternatively, it may be possible to improve on the CKKU construction and eliminate the complex phase altogether. We are particularly interested in the constructions that do not involve a dynamical lattice spacing such as the one that appears here. Many attempts to formulate supersymmetric field theories on the lattice may be found in the literature (see for example [15, 16, 17, 18, 19] and references therein). In our opinion, the recent successes in non-gauge models are very encouraging [20, 21, 22]. Of particular importance is the understanding of these models as “topological” or *Q-exact*, where  $Q$  is an exact supercharge of the lattice system [23, 24, 25]. Indeed, the CKKU undeformed action can be written in a  $Q$ -exact form. An exciting development has been Sugino’s exploitation of this  $Q$ -exact idea to construct lattice super-Yang-Mills with *compact* gauge fields and an ordinary (non-dynamical) lattice spacing [26]. While the Sugino construction has its benefits, he notes (based on a remark by Y. Shamir) that these systems also suffer from a vacuum degeneracy problem that renders the classical continuum limit ambiguous. Consequently, Sugino has introduced a non-supersymmetric deformation in these models that lifts the unwanted vacua; he demands that the relative strength of this deformation be scaled to zero in the thermodynamic limit. Thus in some respects the Sugino construction has a feature that is similar to the models of CKKU. He argues that entropic effects do not destroy the vacuum selection imposed by his deformation. We are currently investigating various aspects of Sugino’s proposal [27].

## Acknowledgements

The author would like to thank Erich Poppitz for comments, especially in regard to the moduli space of the undeformed theory. Thanks are also due to a referee, of an earlier version of this report [14], who provided useful criticism and suggestions. We thank Mithat Ünsal for useful communications. This work was supported by the National Science and Engineering Research Council of Canada and the Ontario Premier’s Research Excellence Award.

## Appendix

## A $\mathcal{N} = 4$ moduli space

Here we establish the well-known solution to (3.3). One way to see this is as follows [28]. First we note that  $S_0$  reduced to the zero modes, which we write as  $S_z$ , takes the form

$$S_z = \frac{N^2}{g^2} \text{Tr} \left( \frac{1}{2} ([x^\dagger, x] + [y^\dagger, y] + [z^\dagger, z])^2 + 2[x, y][y^\dagger, x^\dagger] + 2[y, z][z^\dagger, y^\dagger] + 2[z, x][x^\dagger, z^\dagger] \right) \quad (\text{A.1})$$

Now note that the  $U(1)$  parts of  $x, y, z$  do not appear and can take any value. Thus we can restrict our attention to the  $SU(k)$  parts, which we choose to express in terms of Hermitian matrices  $a_p, b_p$ ,  $p = 1, 2, 3$ :

$$\begin{aligned} x^c T^c &= (a_1^c + ib_1^c) T^c = a_1 + ib_1 \\ y^c T^c &= (a_2^c + ib_2^c) T^c = a_2 + ib_2 \\ z^c T^c &= (a_3^c + ib_3^c) T^c = a_3 + ib_3 \end{aligned} \quad (\text{A.2})$$

Substitution into (A.1) and a bit of algebra yields

$$\begin{aligned} S_z &= -\frac{N^2}{g^2} \text{Tr} \left[ 2 \left( \sum_p [a_p, b_p] \right)^2 + \sum_{p,q} ([a_p, b_q] + [b_p, a_q])^2 \right. \\ &\quad \left. + \sum_{p,q} ([a_p, a_q] - [b_p, b_q])^2 \right] \\ &= -\frac{N^2}{g^2} \sum_{p,q} \text{Tr} ([a_p, a_q]^2 + [b_p, b_q]^2 + 2[a_p, b_q]^2) \end{aligned} \quad (\text{A.3})$$

Using positivity arguments quite similar to those above, one finds that  $S_z \geq 0$  and that  $S_z = 0$  iff

$$[a_p, a_q] = [b_p, b_q] = [a_p, b_q] = 0, \quad \forall p, q \quad (\text{A.4})$$

which is nothing other than Eq. (53) of [28]. Since the matrices are all hermitian and they all commute, it is obviously possible to choose a basis which simultaneously diagonalizes them. This basis will be related to the one used in (A.2) according to  $T^c \rightarrow T'^c = \alpha T^c \alpha^\dagger$ , which is nothing other than the global gauge transformations (3.4).

## References

- [1] A. G. Cohen, D. B. Kaplan, E. Katz and M. Unsal, ‘‘Supersymmetry on a Euclidean spacetime lattice. II: Target theories with eight supercharges,’’ arXiv:hep-lat/0307012.



- [2] J. Giedt, “The fermion determinant in (4,4) 2d lattice super-Yang-Mills,” Nucl. Phys. B **674** (2003) 259 [arXiv:hep-lat/0307024].
- [3] J. Giedt, “Non-positive fermion determinants in lattice supersymmetry,” Nucl. Phys. B **668** (2003) 138 [arXiv:hep-lat/0304006].
- [4] N. Arkani-Hamed, A. G. Cohen and H. Georgi, “(De)constructing dimensions,” Phys. Rev. Lett. **86**, 4757 (2001) [arXiv:hep-th/0104005];
- [5] C. T. Hill, S. Pokorski and J. Wang, “Gauge invariant effective Lagrangian for Kaluza-Klein modes,” Phys. Rev. D **64**, 105005 (2001) [arXiv:hep-th/0104035].
- [6] J. Giedt, E. Poppitz and M. Rozali, “Deconstruction, lattice supersymmetry, anomalies and branes,” JHEP **0303** (2003) 035 [arXiv:hep-th/0301048].
- [7] E. Poppitz, “Deconstructing K K monopoles,” arXiv:hep-th/0306204.
- [8] D. B. Kaplan, E. Katz and M. Unsal, “Supersymmetry on a spatial lattice,” JHEP **0305** (2003) 037 [arXiv:hep-lat/0206019].
- [9] A. G. Cohen, D. B. Kaplan, E. Katz and M. Unsal, “Supersymmetry on a Euclidean spacetime lattice. I: A target theory with four supercharges,” arXiv:hep-lat/0302017.
- [10] H. Georgi and A. Pais, “CP - Violation As A Quantum Effect,” Phys. Rev. D **10** (1974) 1246.
- [11] M. B. Halpern and W. Siegel, “Electromagnetism As A Strong Interaction,” Phys. Rev. D **11** (1975) 2967.
- [12] W. Krauth, H. Nicolai and M. Staudacher, “Monte Carlo approach to M-theory,” Phys. Lett. B **431** (1998) 31 [arXiv:hep-th/9803117].
- [13] G. Munster and M. Plagge, “Study of the complex fermion determinant in a U(1)-L x U(1)-R symmetric Yukawa model,” Phys. Lett. B **301** (1993) 213 [arXiv:hep-lat/9211056].
- [14] J. Giedt, “Deconstruction, 2d lattice Yang-Mills, and the dynamical lattice spacing,” arXiv:hep-lat/0312020.
- [15] G. Curci and G. Veneziano, “Supersymmetry And The Lattice: A Reconciliation?,” Nucl. Phys. B **292** (1987) 555.
- [16] I. Montvay, “Embedding the N=2 supersymmetric Yang-Mills theory in the adjoint Higgs-Yukawa model on the lattice,” Phys. Lett. B **344** (1995) 176 [arXiv:hep-lat/9410015].
- [17] G. T. Fleming, J. B. Kogut and P. M. Vranas, “Super Yang-Mills on the lattice with domain wall fermions,” Phys. Rev. D **64** (2001) 034510 [arXiv:hep-lat/0008009].

- [18] I. Montvay, “Supersymmetric Yang-Mills theory on the lattice,” *Int. J. Mod. Phys. A* **17** (2002) 2377 [arXiv:hep-lat/0112007].
- [19] A. Feo, “Supersymmetry on the lattice,” arXiv:hep-lat/0210015.
- [20] S. Catterall and E. Gregory, “A lattice path integral for supersymmetric quantum mechanics,” *Phys. Lett. B* **487** (2000) 349 [arXiv:hep-lat/0006013].
- [21] S. Catterall and S. Karamov, “A two-dimensional lattice model with exact supersymmetry,” *Nucl. Phys. Proc. Suppl.* **106** (2002) 935 [arXiv:hep-lat/0110071].
- [22] S. Catterall and S. Karamov, “Exact lattice supersymmetry: the two-dimensional  $N = 2$  Wess-Zumino model,” *Phys. Rev. D* **65** (2002) 094501 [arXiv:hep-lat/0108024].
- [23] S. Catterall, “Lattice supersymmetry and topological field theory,” *JHEP* **0305** (2003) 038 [arXiv:hep-lat/0301028].
- [24] S. Catterall, “Lattice supersymmetry and topological field theory,” arXiv:hep-lat/0309040.
- [25] S. Catterall and S. Ghadab, “Lattice sigma models with exact supersymmetry,” arXiv:hep-lat/0311042.
- [26] F. Sugino, “A lattice formulation of super Yang-Mills theories with exact supersymmetry,” arXiv:hep-lat/0311021.
- [27] J. Giedt, E. Poppitz, in progress.
- [28] P. Fayet, “Spontaneous Generation Of Massive Multiplets And Central Charges In Extended Supersymmetric Theories,” *Nucl. Phys. B* **149** (1979) 137.